

© 2020. H.C. Nguyen, D.Q. Ngo.

This is an open-access article distributed under the terms of the Creative Commons Attribution-NonCommercial-NoDerivatives License (CC BY-NC-ND 4.0, <https://creativecommons.org/licenses/by-nc-nd/4.0/>), which permits use, distribution, and reproduction in any medium, provided that the Article is properly cited, the use is non-commercial, and no modifications or adaptations are made.



# FLEXURAL AND SHEAR BEHAVIOR OF REINFORCED CONCRETE BEAMS STRENGTHENED WITH CARBON TEXTILE REINFORCED CONCRETE

H. C. NGUYEN<sup>1</sup>, D. Q. NGO<sup>2</sup>

Recently, textile reinforced concrete (TRC) has been intensively studied for strengthening reinforced concrete (RC) and masonry structures. This study is to experimentally explore the effectiveness of application of carbon TRC to strengthen RC beam in flexure and shear. Concerning the cracks formation, failure modes, ultimate strength and overall stiffness, the performance of the strengthened beams compared to the control beams were evaluated from two groups of tests. The test results confirm that the TRC layers significantly enhance both shear and flexural capacity of RC beams in cracking, yielding and ultimate loads. All of the tested specimens were also modelled using ABAQUS/CAE software, in order to validate the experimental results. The numerical results show that the simulation models have good adaptability and high accuracy.

*Keywords:* textile reinforced concrete, flexural, shear, strengthening, ABAQUS

<sup>1</sup> MSc., Eng., University of Transport and Communications, Faculty of Construction Engineering, 3<sup>rd</sup> Cau Giay str., Hanoi, Vietnam., e-mail: [nguyenhuycuong@utc.edu.vn](mailto:nguyenhuycuong@utc.edu.vn); ORCID: 0000-0002-2235-6679

<sup>2</sup> Prof., PhD., Eng., University of Transport and Communications, Faculty of Construction Engineering, 3<sup>rd</sup> Cau Giay str., Hanoi, Vietnam., e-mail: [ngodangquang@utc.edu.vn](mailto:ngodangquang@utc.edu.vn); ORCID: 0000-0002-5818-8611

## 1. INTRODUCTION

In the recent years, extensive research has been conducted on the strengthening of RC beams with externally bonded Textile Reinforced Concrete (TRC). TRC is the specific type of composite material, consisting of the multiaxial high strength textile embedded in fine grained concrete. TRC is applicable for strengthening existing buildings as well as fabricating new structural elements. Currently, no design codes are yet formalized for TRC, such that many experimental programs are still needed to acquire approval for each individual application.

Experimental and analytical studies of TRC retrofitted RC beams showed that the use of TRC can result in increased moment and shear resisting capacities. A state-of-the-art report by RILEM TC 201-TRC [1] provides guidance for the design of TRC systems for externally strengthened concrete structures, based on experimental research, analytical work. The American ACI 549.4R-13 [3] is currently the only available guideline for design and construction of strengthening systems. Many studies have been carried out to assess the RC beams retrofitted in flexure by TRC through experimental, finite element and analytical approaches (e.g. Brückner et al. [4], Wiberg et al. [5], Babaeidarabad et al. [6], D'Ambrisi et al. [7], Hussein et al. [8], Sneed et al. [9]). All of these studies showed results that that the application of TRC can increase in load carrying capacity of strengthened elements/structures considerably. In these studies, the key parameters were analysed, including textile reinforcement ratio (expressed by the number of layers), steel reinforcement ratio, material properties, strengthening configuration. By increasing the amount of applied textile reinforcement, flexural capacity increases. However, this correlation is not consistent due to different failure modes in strengthened structures. There are three primary types of bond failure associated with TRC system, including slippage of rovings [7], detachment of TRC from concrete substrate [8] and delamination within the TRC mortar and textile reinforcement [7]. These brittle failure modes control the strengthening effectiveness, resulting in low level of strengthening. D'Ambrisi et al. [7] and Sneed et al. [9] tried to improve the effectiveness of the strengthening layers by providing anchorage with the use of additional TRM U-strips at the full length or only at the two ends of the strengthening layers. According to their results, there was no strong evidence that the extra measures helped to increase load-carrying capacity.

Only few researchers [10-17] have investigated the use of TRC for shear strengthening of RC beams. Parameters such as the number of layers, fabric type, type of mortar layers, and the strengthening

configuration have been investigated. In particular, Escrig et al. [15] investigated the shear performance of beams strengthened with different textile material, including basalt, carbon, PBO, and glass. It was concluded that the bond between the mortar and the textile used and also the bond between the TRC and the concrete substrate significantly affect the performance of the TRC system. Tetta et al. [16] concluded that U-shaped jackets exhibited much more effective than side-bonded jackets in increasing the shear capacity of beams. Blanksvärd et al. [12] strengthened RC beams using TRC made of different types of mortars and carbon textile. Blanksvärd reported that using mortars with higher mechanical properties along with the incorporation of fibers could improve the performance of TRC systems. Contamine et al. [14] tested two average TRC thicknesses in strengthening damaged RC beams and concluded that the thickness of reinforcement did not significantly affect the strength gains of the strengthened specimens.

There is no doubt that TRC systems have proven mechanical and structural performance but, because it is a relatively new material, its full potential has yet to be validated. Due to the short history of research on use of TRC composites for structural strengthening, the number of research studies on RC beams strengthened both in flexure and shear is limited compared to studies concentrating only one of them. These studies also showed sometimes inconsistent conclusions due to the wide variety in the properties of TRC systems used, especially the unstable in bond properties between textile rovings and fine grained concrete. The overarching goal of this study was to explore the effectiveness of carbon TRC for use in strengthening RC beams in flexure and shear. A total of twelve beams were fabricated and strengthened with carbon TRC. In addition to the experimental program, a numerical investigation utilizing nonlinear FE analysis was developed to predict the load-carrying capacity and response of RC beams strengthened both in flexure and shear with TRC.

## 2. EXPERIMENTAL PROGRAM

### 2.1. TEST SPECIMENS

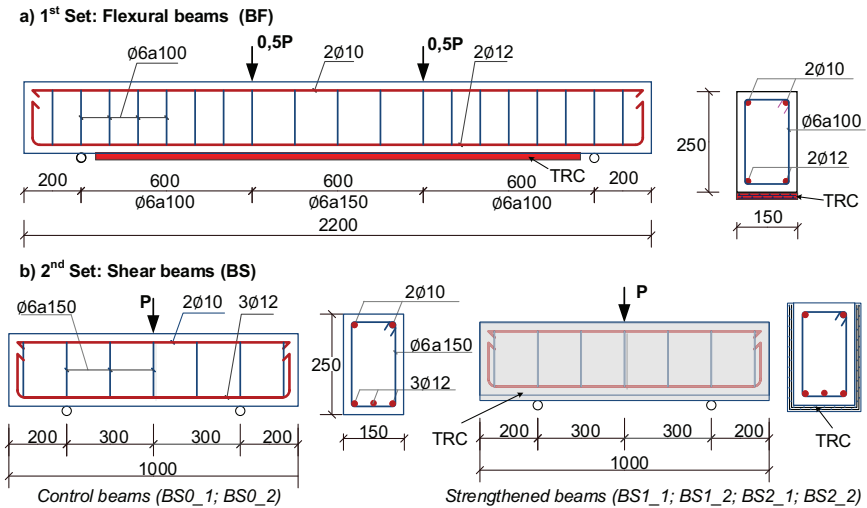


Fig. 1. Detail of test beams

The objective of the test program was to investigate the flexural and shear performances of strengthened beams loaded up to failure. This includes load – deflection behavior, crack patterns, ultimate capacities, and modes of failure. Two sets and a total number of 12 reinforced rectangular concrete beams were cast and tested. The cross section of the beams was 150 mm x 250 mm, as shown in Fig. 1. The beam in set 1 was 2200 mm long and was supported over a clear span of 1800 mm during testing. These beams were reinforced with two  $\phi 12$  tensile reinforcing bars, and were tested under four points bending test. Two of them, denoted as BF0\_1 and BF0\_2, were control beams and the other four were strengthened with carbon textile reinforced concrete. Two beams, namely BF1\_1 and BF1\_2, were strengthened with 1 layer of carbon textile. The remaining two beams, BF2\_1 and BF2\_2, were upgraded with 2 layers of carbon textile.

In set 2, the tensile reinforcement used was increased to three  $\phi 12$  bars. These beams were 1000 mm long, with 600 mm clear span and were tested under three points bending test. Two beams (BS0\_1 and BS0\_2) were the control beams, and the other four was strengthened with 1 and 2 layers of carbon textile, in form of U-wraps. These beams were subjected to the three points bending test. Two  $\phi 10$  bars were provided as the compression reinforcement in all two sets of beams.

## 2.2. MATERIALS SPECIFICATION

All beam specimens were fabricated using normal strength concrete. The concrete used to manufacture all beams was mixed, cast and cured in the laboratory. The measured cylinder compressive strength of the concrete used for the beams was 39.5 MPa. The yield stress of the longitudinal reinforcing steel was 293 MPa, while the stirrups steel had the yield strength of 235 MPa. The fine grained binder systems with a maximum grain size of 0.6 mm was specifically designed for application with carbon textile, was comprised of high-fineness cement binder. The high performance plasticizer and fly ash were added to achieve a very good flowing capability of the concrete in order to ensure a proper penetration of the small gaps of the fabrics. The fine grained concrete was mechanically characterized by testing six 40 mm × 40 mm × 160 mm prisms. The obtained average flexural strength and average compressive strength at 28 days were equal to 8.5 MPa and 70.1 MPa.

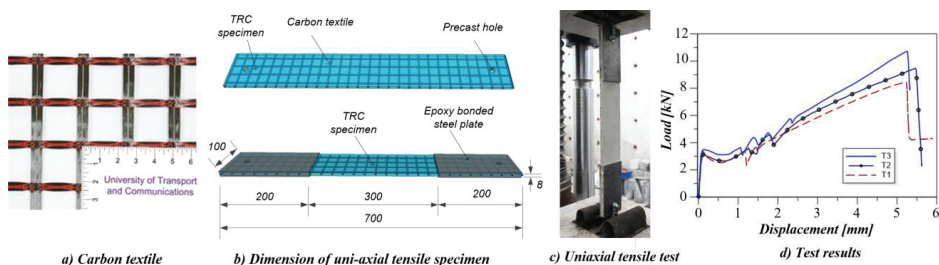


Fig. 2. Uni-axial tensile test for TRC specimen

The carbon textile product Sigratex Grid 350 with a fineness of 1600 tex was used in this study. The distance between the rovings is 25 mm in longitudinal direction as well as transversal direction (Fig. 2-a). The tensile strength and elastic modulus of the fiber were measured by means of tensile tests on bare roving coupons (i.e. not impregnated by the fine grained concrete) and were equal to 3550 MPa, and 225 GPa, respectively. The tensile strength of the textile roving was also determined by the uni-axial tensile tests on the specimen with dimensions of 8 × 100 × 700 mm (Fig. 2-b,c,d). In manufacturing the specimen, first a 4-mm thick layer of the fine grained concrete was applied, then a layer of textile was placed and lightly pushed into the first layer of matrix. Eventually the top layer of fine grained concrete was applied to form the surface of the specimen. Four steel tabs were attached to the ends of each coupon with high strength epoxy. The averaged tensile strength of textile reinforcement was equal to 3358 MPa. The typical load-displacement curve in tensile test is also displayed in Fig. 2-d. The test results indicated that TRC plate exhibit distinct strain-hardening

behavior, with the classic three-stages, including: non-cracked stage, crack stabilization stage, and failure stage.

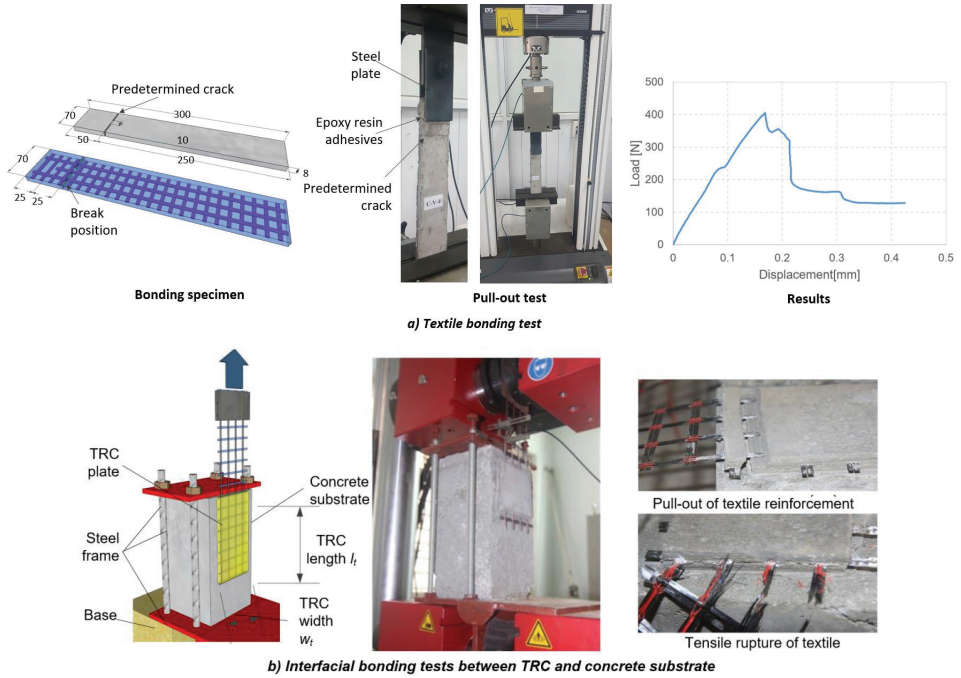


Fig. 3. Test setup for determining mechanical properties of TRC

For preparing this experiment, a series of basic tests were carried out to obtain the mechanical properties of TRC layers, including: bond behavior between carbon textile and fine grained concrete; interfacial bond behavior between TRC and substrate concrete (Fig. 3). The bond behaviour between textile reinforcement – fine grained concrete is very important for the whole load bearing behaviour of the TRC structures. Based on the pull-out test recommended by Approval Z-31.10-182 [2], one-layer reinforced specimens measuring 300 mm × 70 mm × 8 mm with a predetermined crack is prepared. Per specimen, exactly one roving with embedment length of  $l_{E,0} = 25$  mm can be gradually pulled out from the fine grained concrete (Fig.3-a). The average bonding strength between carbon textile and fine grained concrete was 19.6 N/mm (force per length). Based on the tested results, the effective anchorage length of textile in fine grained concrete can be calculated as about 160 mm. The interfacial behavior is commonly studied through a pull-out test in which a TRC plate bonded to a concrete prism is subjected to tension, developed within RILEM TC 250-CSM [19] (Fig. 3-b). The

average bonding strength between TRC and concrete substrate was approximately 5.4 MPa.

### 2.3. SPECIMEN CONFIGURATION AND INSTRUMENTATION

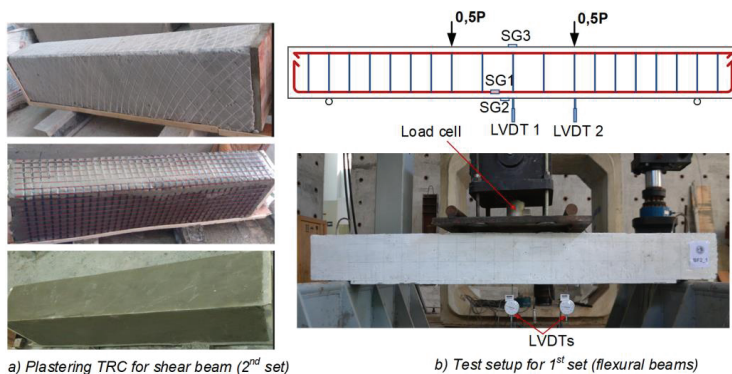


Fig. 4. Strengthening steps and view of the test set-up

All RC beams were air cured at indoor conditions for 28 days before strengthening. Then, RC beams in each sets were selected to strengthen with carbon TRC. In order to achieve desired composite action between the RC beams and the strengthening system, the surfaces which were going to have the TRC applied were roughened to improve the adhesion performance. Then, in the first set, the TRC layer with 1700 mm length and 150 mm width were bonded to tension surface of RC beams. Each textile layer consists six rovings with  $5.28 \text{ mm}^2$ . Similarly, the shear beams in set 2 were fully strengthened in form of U-jackets. After the 28-day period, all beams in 2 sets were tested. It should be noted that, the averaged compressive strength of concrete beam at the test day was recorded as 43.2 MPa. All beams were tested using displacement controlled method, with loading rate of 1 mm/min. Schematic view and a view of the test setup are shown in Fig. 4. Two LVDTs were installed on the bottom surface of the beams to measure their deflections during the test. Moreover, strain gages were used to record concrete strains at surfaces and steel reinforcement during the experiment. All the tests were conducted in the Structural Engineering Laboratory at University of Transport and Communications, Vietnam.

### 2.4. EXPERIMENT RESULTS

Table 1 shows a summary of the flexural behavior of all test beams in terms of flexural loading capacity, mid-span deflection and failure modes. Load versus mid-span displacement curves are presented as shown in Fig. 5 for all test beams. In addition, final modes of failure and crack patterns are illustrated in Fig. 6.

Table 1. Load and modes of failure comparison for flexural beams in Set 1

Beam	Cracking		Yielding		Ultimate		Failure mode
	Load $P_{cr}$ (kN)	Deflection $D_{cr}$ (mm)	Load $P_y$ (kN)	Deflection $D_y$ (mm)	Load $P_u$ (kN)	Deflection $D_u$ (mm)	
BF0_1	13.33	0.22	59.28	4.95	71.84	40.45	Flexure
BF0_2	12.50	0.16	57.09	3.79	72.68	38.40	
BF1_1	15.50	0.37	65.18	4.23	88.64	30.35	Textile rupture
BF1_2	16.67	0.33	66.55	4.10	90.28	27.10	
BF2_1	18.33	0.31	67.83	3.35	104.69	27.40	
BF2_2	19.50	0.38	70.25	4.15	101.12	24.35	

The experimental testing began with the control beam BF0\_1 and BF0\_2 in Set 1. As shown in Fig. 5, these specimens displayed the standard nearly-bilinear response behaviour. Three regions can be clearly identified, including pre-cracked stage, post-cracked stage and post-yielding stage. The load – displacement curves indicate a linear elastic behaviour, up to the point of first crack. The first cracks occurred at a loading of about 13.33 kN and 12.50 kN, respectively. Stiffness of the beams decreased after the first cracks, resulting in larger deflection. That was followed by nonlinear load-deflection response when further increments of load were applied until the beams failed. The yielding of the steel reinforcement occurs at a load of 59.28 kN (BF0-1) and 57.09 kN (BF0-2). After yielding of tensile reinforcement, the applied load remains almost constant until it drops considerably once concrete crushes in compression. The average ultimate load and mid-span deflection of the two beams were 72.26 kN and 39.4 mm, respectively. The two reference beams failed in flexure due to the yielding of the tensile steel reinforcement followed by the concrete crushing. The formation of wide flexural crack at the mid-span was presented in Fig. 6-a.

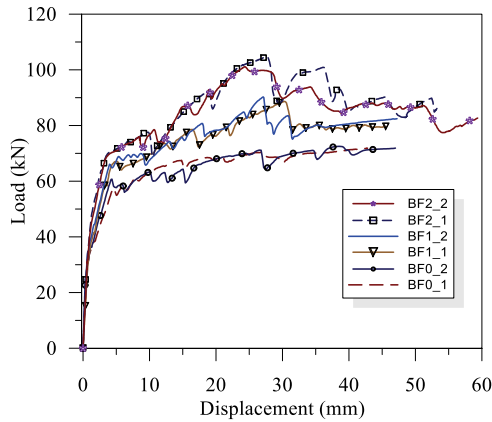


Fig. 5. Load–mid span displacement curves for flexural beams (Set 1).

All strengthened beams had similar behavior as that of control beams. At earlier stages (i.e. before flexural cracking), the load–displacement curves are close to each other. The specimens exhibit a linear load–deflection behavior prior to the cracking of concrete. A slightly greater cracking load is observed at the beams strengthened with TRC due to the larger cross sectional area. After cracking, the strengthened specimens exhibited larger stiffness compared to the control beams. A considerable increase of the measured yielding load was observed due to the addition of the TRC layer for the strengthened beams BF1\_1, BF1\_2, BF2\_1 and BF2\_2, as shown in Table 1. The yielding loads of the strengthened beams were 65.18, 66.55, 67.83 and 70.25 kN, respectively. After yielding of reinforcing bars, major increase in tension force was transferred to the carbon textile. The strength and stiffness of the strengthened specimens were larger compared to the control specimens. The post-yielding branch of the load-deflection diagram continues up to the loss of strengthening action due to textile rupture. As it was expected, the presence of the strengthening system significantly increases the flexural strength of beams, in terms of ultimate load. From Table 1, it is noted that the percentage strength increases over the control member range from a minimum value of 25%, when using a single layer of carbon textile, to a maximum of 43% in the case of TRC system with 2 layers of carbon textile. After rupture of textile, the load–displacement curve of the strengthened specimens dropped and almost corresponded to those of the control beams. The load level stayed at approximately 80 kN after dropping down from the maximum value of 104.69 kN.

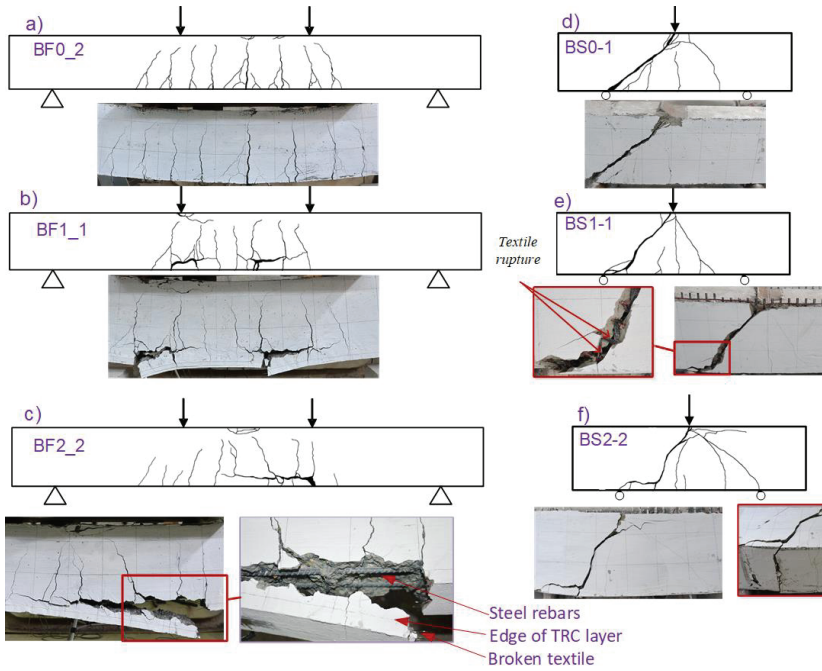


Fig. 6. Crack patterns of flexural and shear beams at failure

All strengthened beams failed due to the sudden tensile rupture of carbon textile, accompanied by a loud noise. Severe crushing of concrete occurred under the loading point. Cracks width in strengthened beams were substantially narrower than ones observed in the control beams. The cracks continued to extend, opened and branched until failure of the beams. Peeling failure of the concrete cover along the steel reinforcement level adjacent to the external TRC layer occurred for all strengthened beams. A crack initiated in the positions of the textile rupture, then developed to the level of the tension steel reinforcement, and propagates horizontally towards the mid span, forming “teeth” between the cracks (Fig. 6-b,c). The TRC layer is gradually peeled off with lumps of concrete detached from the longitudinal steel rebar. It should be noted that there was no horizontal bond crack in the bonding surfaces between TRC and concrete substrates. Therefore, the adhesion performance was sufficient enough to safely transfer tensile loads from the TRC strengthening layer to the concrete substrate.

Set 2 consists of two control beams and four beams strengthened in shear with carbon TRC. The experimentally obtained load deflection curves of the beams in this set are plotted in Fig. 7. This figure also provides a summary of the test results including loads and mid-span deflections at ultimate capacity, together with observed modes of failure. In general, all six shear beams had a similar failure

process with diagonal shear cracking initiated in the shear span regions. The diagonal cracks then increased dramatically and propagated toward the top area and develop across the spans with increasing load. The shape and pattern of cracking are shown in Fig. 6-d,e,f.

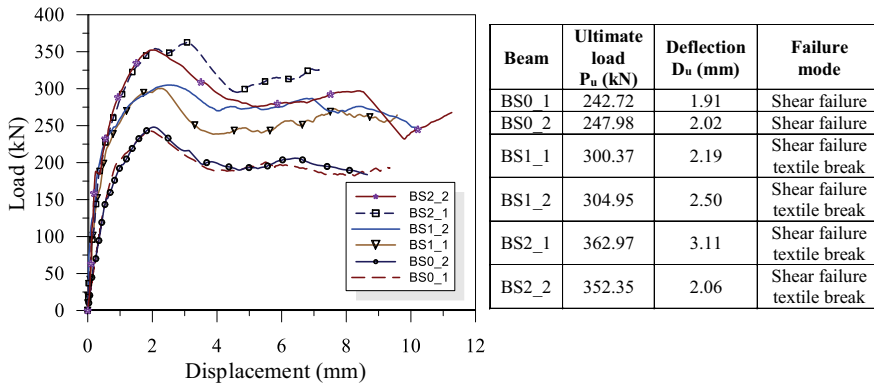


Fig. 7. Load – displacement relationship of shear beams in Set 2

The behavior of BS0\_1 and BS0\_2 specimens presented a typical shear failure mode, consisted of three stages namely: (a) the non-cracked stage, (b) the cracked stages and (c) the failure stage. The first visual shear cracks for the control specimens form in the center of the load span. After cracking, the load still increased with the smaller stiffness, due to the aggregate interlocking effect and the dowel action of the longitudinal rebars. The beams failed gradually and then the cracks developed until the ultimate load applied. After that, the load dropped to the smaller load level (194 kN).

For the strengthened beams BS1-1 and BS1-2, the first crack occurred at a load higher than that of the control specimens. Due to the section enlargement with TRC, the initial stiffness of strengthened beams was also higher than that of reference specimens. The first small visual shear crack appeared in a load range of 172–179 kN. The shear crack became larger and larger with increased deflection and the beams failed by plate-end shear at about 300 kN. The shear capacities of the beam BS1\_1 were about 24.5% more than their un-strengthened beams. Failure occurred due to extension of the large diagonal shear crack and the tensile break of transverse textile rovings, and the load fluctuated at level of 250 kN. The remaining load in the strengthened beams was much higher than that of the control beams, due to the existence of pull-out textile rovings. At the diagonal crack, the transverse filament yarns with very long bond lengths failed by tensile break, while yarns with short bond lengths failed by complete pull-out. These pull-out textile rovings could carry a small tensile load due to the friction between the roving and fine grained concrete.

Similarly, strengthening by 2 layers of U-wraps of textile provides a 41.6% increase in shear bearing capacity compared to the non-strengthened reference specimen. It should be noted that, critical diagonal crack associated with the shear failure occurred in all specimens, while the crack angles were in the range 37 to 55 degrees with respect to the horizontal. The crack angles of the beam BS2-1 and BS2-2 were higher than both control beam and the beam BS1-1 and BS1-2, since the amount of textile reinforcement provided was larger. These diagonal cracks extended and gradually peeled off with concrete cover detached from the longitudinal steel rebar Fig. 6-e, f.

### 3. NUMERICAL INVESTIGATION

#### 3.1 FE MODELING

The numerical analysis using ABAQUS 6.12-1 software was carried out to predict not only the ultimate load bearing capacity, but also the mechanical behavior of the structures, and then compared to the measured results. A total of six FE models was performed for both flexural and shear specimens. A full view of specimen BF1-FEM is shown in Fig. 8 for reference. Due to the symmetry of the specimen geometry and loading, in order to save the calculation time, only half of the specimens were modelled. The beam was restrained at the support by means of hinges. The loading was applied continuously in the form of the displacement control manner.

Four components of specimen (concrete beam, steel rebar, fine grained concrete layer, and textile reinforcement) was modelled separately and assembled to make a complete specimen model. The steel bars and textile are embedded into the concrete by embedded constraints, which implies infinite bond strength at the interface between the concrete and the reinforcement. In order to connect the concrete beam with the fine grain concrete layer, the surface-based tie constraint is used. The experimental results mentioned above have shown that the bonding between the two concrete surfaces is strong enough and a delamination of the fine grain concrete is not to be expected. Therefore, these two parts are tied together without any relative motion. The element type used for the numerical discretization in the 3D concrete parts is the C3D8R element from the ABAQUS library. modelled using solid, beam or truss elements. The T3D2 (3-noded quadratic 2-D) truss elements are used for the reinforcement bars and textile. The reinforcement was modelled with the wire-option in ABAQUS. Fig. 8 also shows the meshing of the FE model for the concrete beam, rebar, fine grained concrete layer and carbon textile. In order to achieve the reliable results, the fine mesh was used in the pure bending zone.

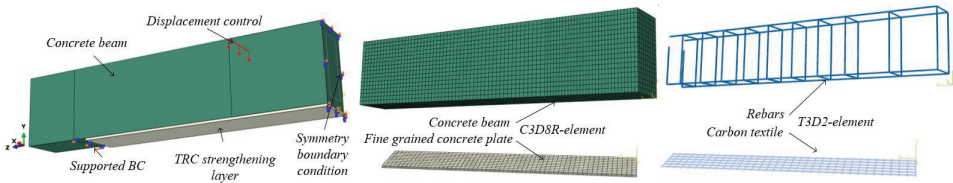


Fig. 8. FE model of RC beam strengthened with TRC layer in flexure (BF1-FEM)

The longitudinal and transversal steel bars were modelled with an elastic–plastic model. In the linear elastic range the behavior was defined by Young modulus (200 GPa) and the Poisson’s ratio (0.3); whereas in the plastic range it was modelled according to the experimental data (Fig. 9-a). The ultimate strength of steel reinforcement was 428 MPa, which was obtained from the experimental test. The model for both compression and tension is assumed to be identical.

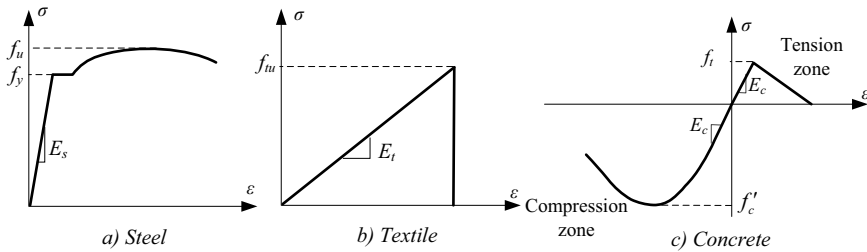


Fig. 9. The stress-strain relationship for the steel, textile, and concrete materials.

The material behaviour of single textile roving can be appropriately described with a brittle elastic isotropic material. As seen from Fig. 9-b, the textile material was captured the response of elastic-brittle materials, and it showed that there is no appreciable plastic deformation before failure. The stress is linear up to the tensile strength, and do not exhibit the yielding behavior. After reaching the tensile strength, the stress drops sharply to zero, representing the rupture of textile. The input parameters were assigned according to the experimental data.

The Concrete Damaged Plasticity (CDP) model, was adopted to model the inelastic stress-strain relation in the compressive and tensile regions (Fig. 9-c). For compressive behavior, the elastic modulus and the uniaxial stress-strain curve of were calculated according to Eurocode 2 [18], and were selected for the determination of yield stress and inelastic strain. For tensile behavior of

concrete, the tensile stress was assumed to increase linearly with respect to the strain until the concrete crack. After the concrete crack, tensile stress decreases linearly to zero. The value of the strain at zero stress can be taken as 10 times the strain at failure as suggested in ABAQUS manual. In the CDP model, there are five additional parameters describe the yield surface, potential flow, and visco-plastic regulation, respectively. Two parameters  $\frac{\sigma_{b0}}{\sigma_{c0}}$  and  $K_c$  are used to modify the yield surface. Two other parameters modify the non-associated potential flow: dilation angle  $\psi$  and eccentricity of the potential flow  $c$ . The viscosity coefficient  $\mu$  were set to a small value, which helps to improve the rate of convergence of the model. The default values of these parameters are taken as recommendation of CDP model in ABAQUS user's manual [18]. These material properties have been assigned in CDP model are summarized in Table 2.

Table 2. The values of the parameters used in CDP model for concrete

Concrete type	$f_c$ (MPa)	$f_{cr}$ (MPa)	$E_c$ (MPa)	$\nu$	$K_c$	$c$	$\frac{\sigma_{b0}}{\sigma_{c0}}$	$\psi$	$\mu$
Normal	39.5	3.47	33090	0.2	2/3	0.1	1.16	30°	1E-5
Fine-grained	70.1	8.5	39520	0.2					

### 3.2 VERIFICATION OF THE FE MODEL

In order to verify the FE model, the numerical and experimental load-deflection curves obtained for the beams are compared with each other and illustrated in Fig. 10 and Fig. 11. A comparison was made between the ultimate loads obtained from the experimental and the numerical studies for all beam specimens was summarized in Table 3 for both sets.

As can be seen in Fig. 10, all three FE beams in Set 1 are slightly stiffer than the actual beams in the linear range. This can be explained by the bond between the concrete and reinforcements is assumed to be perfect (no slip) in the FE analyses. For the actual beams, the assumption would not be true and some slip occurs, therefore the composite action between the concrete and steel reinforcing is lost in the actual beams. It is noted that the failure modes predicted from the FE analysis matches very well with the experimental observations. The control beam BF0-FEM failed due to yielding of the steel followed by concrete crushing, while beams BF1-FEM and BF2-FEM failed by textile rupture at mid-span after the textile attained its maximum stress.

Table 3. Comparison of experimental and numerical results

Beam	Set 1 - Flexural strengthening						Set 2 - Shear strengthening			
	Yielding load $P_y$ (kN)			Ultimate load $P_u$ (kN)			Beam	Ultimate load $P_u$ (kN)		
	EXP	FEM	EXP/FEM	EXP	FEM	EXP/FEM		EXP	FEM	EXP/FEM
BF0_1	59.28	58.34	1.02	71.84	69.87	1.03	BS0_1	242.72	236.87	1.02
BF0_2	57.09		0.98	72.68		1.04	BS0_2	247.98		1.05
BF1_1	65.18	64.33	1.01	88.64	83.47	1.06	BS1_1	300.37	308.49	0.97
BF1_2	66.55		1.03	90.29		1.08	BS1_2	304.95		0.99
BF2_1	67.83	70.15	0.97	104.69	92.83	1.13	BS2_1	362.97	337.86	1.07
BF2_2	70.25		1	101.12		1.09	BS2_2	352.35		1.04

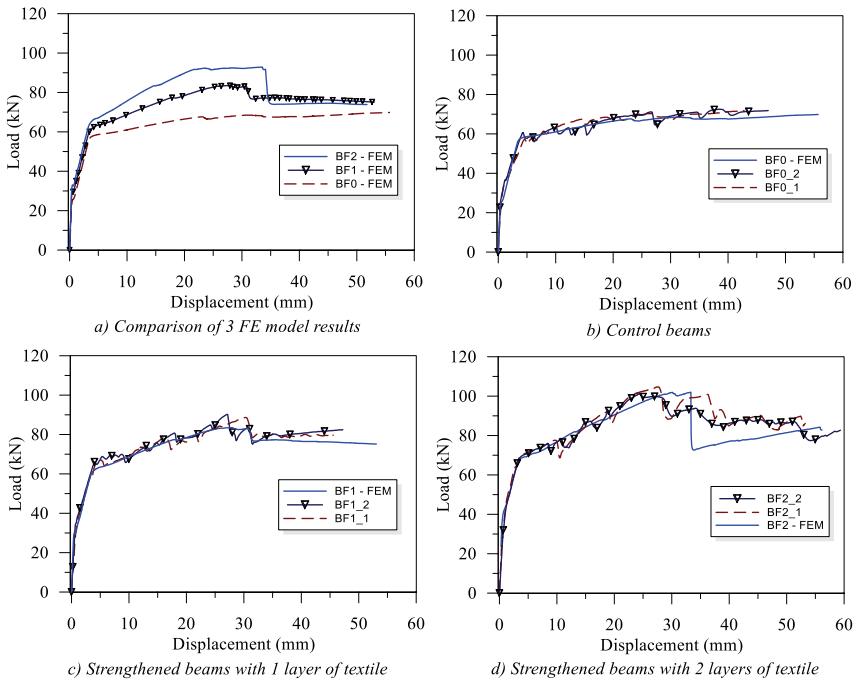


Fig. 10. Comparison of numerical and experimental results of the flexural strengthened beams in Set 1

The non-strengthened numerical model shows a very similar behaviour compared to the experimental results. The yielding of the steel reinforcement starts at the same load level as at the experiments. Further on, the curve of the model runs parallel to the curves obtained in the tests. At a deflection of 22 mm, a small drop appears, representing the crushing of concrete in compression zone. After this

point the curve recovers slightly but the capacity cannot be increased significantly anymore. The strengthened models (namely BF1-FEM and BF2-FEM) behave in the same manner. The first concrete tension cracks occur almost at the same time at 24 kN, while the yielding of the steel starts slightly earlier. After the maximal moment value of the model is reached, the curve drops to the same load level as the test beams. Average discrepancy in peak load values between experimental and FE predictions was found to be about 7% and 11%, respectively. After this point, the experimental curves show a lot of small drops, due to the non-uniform distribution of load in the longitudinal rovings, leading to the continuous failures of one or more bundles. The FE model runs smoother in comparison, because all the longitudinal rovings broke at the same time.

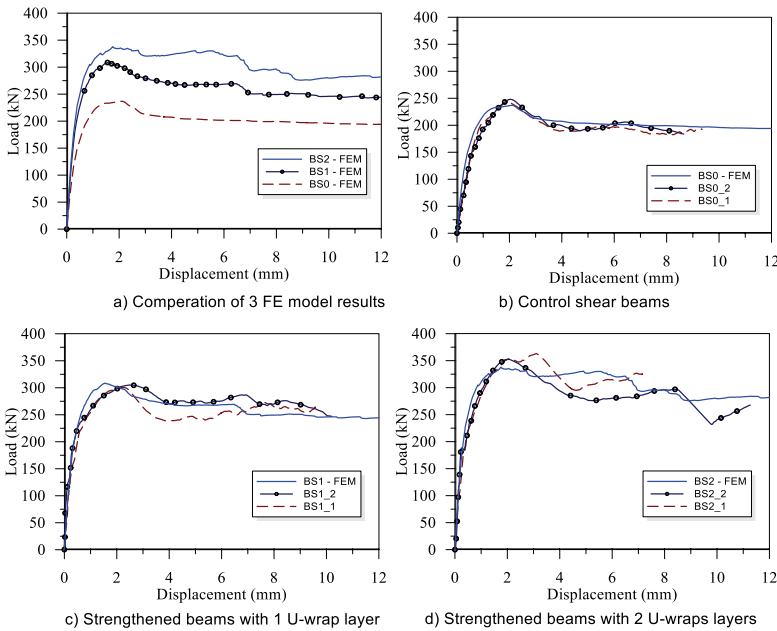


Fig. 11. Comparison of numerical and experimental results of the shear strengthened beams in Set 2

The numerical results for shear strengthened beams in Set 2 are plotted in Fig. 11 and compared with the experimental data by the load–displacement curves. It could be concluded that, the load–displacement diagram from FE analysis agrees well with the experimental results, with deviation of 1–7%, and final collapsed modes of all beams are consistent. In the initial stages of loading, the stiffness of the numerical models is marginally higher than experimental results. After reaching the

ultimate load, the load decreases gradually in the subsequent period.

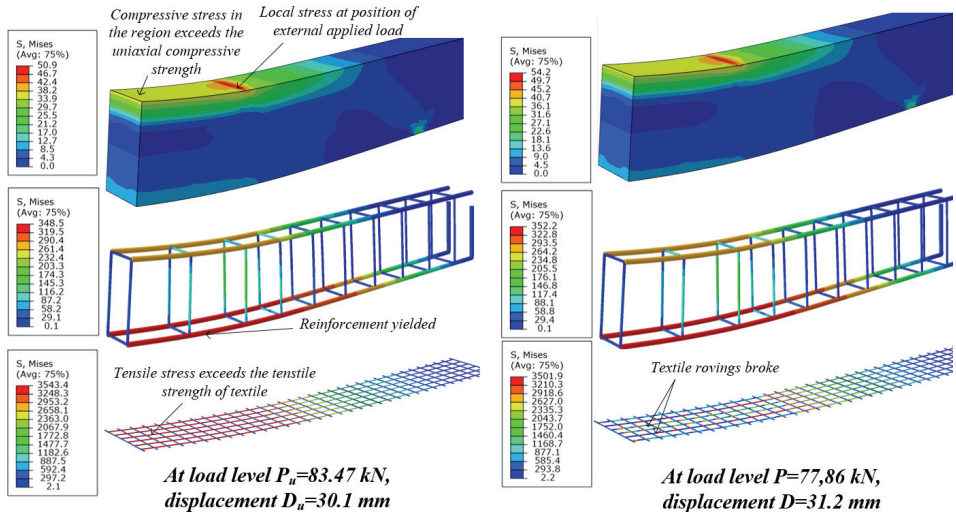


Fig. 12. Von Mises stress distribution in concrete, rebars and textile in BF1-FEM model

In detail, the breaking of carbon textile in BF1-FEM model is also numerically depicted by the Von Mises stress distribution as shown in Fig. 12. As can be seen, at the applied load of 85.69 kN, the tensile stresses of carbon layer in pure flexural zone exceeded the tensile strength of textile. Then, with the increase of the applied displacement, tensile stress of textile at these positions dropped suddenly to zero, representing the rupture of textile reinforcement. It is also noted that some crushing zones are indeed observed in concrete before reaching the breaking of textile in tension. It shows the well agreement in failure mode to the experiment results.

Using these verified FE models, a parametric analysis was carried out to examine the effects of the steel reinforcement ratio on the overall behavior of strengthened beams. In the experimental program, the control beams were reinforced with 2 rebars of 12 mm diameter as tension reinforcement, corresponding to the flexural reinforcement ratio of 0.68%. In the parametric study, the tensile reinforcement diameter is changed from 12 mm to 16 mm and 20 mm, corresponding to  $\rho = 1.21\%$  and 1.90%, respectively. The load versus deflection relationship for the different reinforcement ratios is shown in Fig. 13. The ultimate load-bearing capacities and the strengthening factor (SF) are also displayed in Fig. 13. From the observation, it could be said that the reinforcement ratio has a significant influence on the flexural strength and failure mode of the strengthened beams. The model

with lower reinforcement ratio results has the lowest stiffness after cracking, as well as the lowest ultimate load capacity. This may be attributed to the fact that as the diameter of the rebars increases, the ultimate loading capacity of the strengthened beams increases. However, when the reinforcement ratio increases, all the beams are failed by concrete crushing. Thus, the contribution of TRC in strengthened beams decreases as the reinforcement ratio increases. With a reinforcement degree of  $\rho = 1.21\%$  ( $d = 16 \text{ mm}$ ) each layer of TRC only gains a strengthening effect of 8%. This drops to 3% if 20 mm rebars are used ( $\rho = 1.90\%$ ). It becomes clear that nearly no strengthening effect is generated by adding layers of TRC.

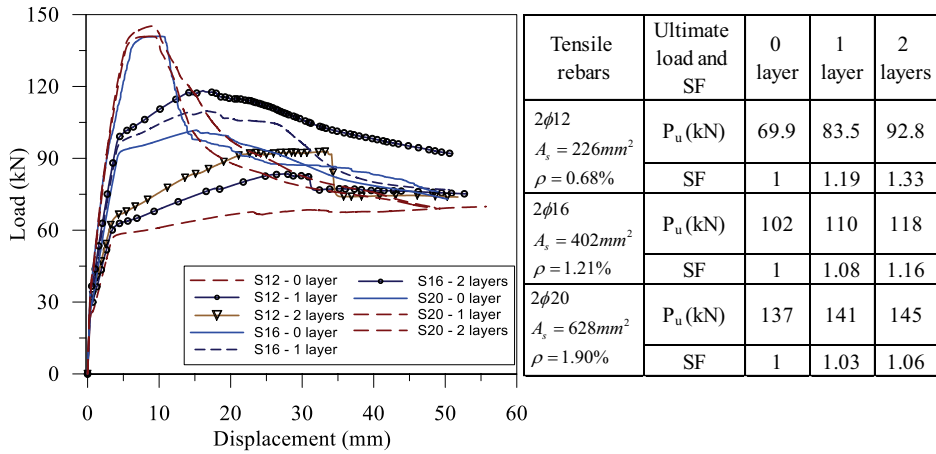


Fig. 13. Flexural behavior of the numerical models ran with different steel reinforcement ratios

When tensile rebars with a diameter of 16 mm are used, the capacity of strengthened beams slightly increased after the steel reinforcement starts yielding. After the ultimate capacity is reached, the concrete zone fails successively. The capacity of strengthened beams increase slightly but the full capacity of the textile material could not be used. When the model is run with a steel diameter of 20 mm, this effect becomes even clearer. After yielding of steel reinforcement, the load increases minimally in the a short-term. After the ultimate capacity is reached, the load drops dramatically due to an abrupt failure of the concrete zone. By adding layers of textile reinforcement, the stiffness of the strengthened beams increased marginally and gained a slightly higher ultimate load value, however the failure mode did not change. This type of failure shows that, the effect of the tensile reinforcement ratio is important in the ductility and the effectiveness of the strengthened beams, due to the limitation of concrete strength. If the amount of steel reinforcement is high while the capacity

of concrete zone is undersized, no significant strengthening effect is reached by adding TRC.

## 4. CONCLUSION

The main purpose of the study was to determine the effectiveness of TRC for strengthening the RC beams in both flexure and shear. As expected, strengthened beams presented a significant increase of the ultimate load comparing to the control beams. With two layers of textile reinforcement, an increase of the flexural capacity up to 43% could be reached. Similarly, the shear capacity of RC beam strengthened with 2 layers of U-wraps provides a 41.6% increase compared to the reference specimens.

The adhesion performance was sufficient enough to safely transfer tensile loads from the TRC strengthening layer to the concrete substrate. All flexural strengthened beams in set 1 failed due to the rupture of the textile reinforcement, resulting in peeling failure of the concrete cover along the steel reinforcement level. In set 2, some of the transverse filament yarns with short bond lengths failed by complete pull-out, did not fully carry tensile strength for shear load.

The proposed FE model was capable for accurately predicting the load-carrying capacities and load-deflection relationships for the RC beam as well as the strengthened beams. Average discrepancy in peak load values between experimental and FE predictions was found to be about 1–11%, and final failure modes of all beams are consistent. A parametric study was then conducted, and it can be said that the effect of strengthening decreases with the increase of steel reinforcement ratio. The concrete compression zone failed abruptly which made it impossible to increase the beam capacity by adding TRC.

**Acknowledgments:** This research is funded by university of transport and communications (utc) under the project code t2019-ktxd-07td.

## REFERENCES

1. W. Brameshuber, "Textile Reinforced Concrete. State-of-the Art," Report of RILEM Technical Committee 201-TRC, 1st ed. Bagnaux, vol. 36: RILEM Publications S.A.R.L., ISBN 2-912143-99-3, 2006.
2. Zulassung Z-31.10-182, "Gegenstand: Verfahren zur Verstärkung von Stahlbeton mit TUDALIT (Textilbewehrter Beton)," Prüfstelle: DIBt, Antragsteller: TUDAG TU Dresden Aktiengesellschaft, 2015
3. ACI Committee, "ACI 549.4R-13: Guide to Design and Construction of Externally Bonded Fabric-Reinforced Cementitious Matrix (FRCM) Systems for Repair and Strengthening Concrete and Masonry Structures," American Concrete Institute, 2013.
4. A. Brückner, R. Ortlepp, M. Curbach, "Textile reinforced concrete for strengthening in bending and shear",

- Materials and Structures, Volume 39, Issue 8 , pp 741-748, 2006.
5. A. Wiberg, "Strengthening of Concrete Beams Using Cementitious Carbon Fibre Composites," Doctoral thesis, Royal Institute of Technology, Stockholm, Sweden, 2003.
  6. S. Babaeidarabad, G. Loreto, and A. Nanni, "Flexural Strengthening of RC Beams with an Externally Bonded Fabric-Reinforced Cementitious Matrix," *Journal of Composites for Construction*, Volume 18, Issue 5, 2014.
  7. A. D'Ambrisi and F. Focacci, "Flexural Strengthening of RC Beams with Cement-Based Composites," *Journal of Composites for Construction*, Volume 15, Issue 5, 2011.
  8. M. E. Hussein, T. H. Almusallam, S.H. Alsayed, Y.A. Al-Salloum, "Flexural strengthening of RC beams using textile reinforced mortar – Experimental and numerical study," *Composite Structures*, Volume 97, March 2013, pp 40–55, 2013.
  9. L. H. Sneed, S. Verre, C. Carloni, L. Ombres, "Flexural behavior of RC beams strengthened with steel-FRCM composite", *Engineering Structures*, Vol 127, pp 686-699, 2016.
  10. T. C. Triantafillou and C. G. Papanicolaou, "Shear strengthening of reinforced concrete members with textile reinforced mortar (TRM) jackets", *Materials and Structures*, 39(1), pp 93-103, 2006.
  11. A. Brückner, R. Ortlepp and M. Curbach, "Anchoring of shear strengthening for T-beams made of textile reinforced concrete (TRC)", *Materials and Structures*, Volume 41, Issue 2, pp 407-418, 2008.
  12. T. Blänksvard, B. Täljsten and Carolin A, "Shear strengthening of concrete structures with the use of mineral based composites", *Journal of Composites for Construction*, 13(1), pp 25-34, 2009.
  13. A. Si Larbi, R. Contamine, E. Ferrier and P. Hamelin, "Shear strengthening of RC beams with textile reinforced concrete (TRC) plate", *Construction and Building Materials*, 24(10), pp1928-1936, 2010.
  14. R. Contamine, A. Si Larbi and P. Hamelin, "Identifying the contribution mechanisms of textile reinforced concrete (TRC) in the case of shear repairing damaged and reinforced concrete beams", *Engineering Structures*, Vol 46, pp 447-458, 2013.
  15. C. Escrig, L. Gil, E. Bernat-Maso and F. Puigvert, "Experimental and analytical study of reinforced concrete beams shear strengthened with different types of textile-reinforced mortar", *Construction and Building Materials*, Vol 83, pp 248-260, 2015.
  16. Z. C. Tetta, L. N. Koutas and D. A. Bournas, "Textile-reinforced mortar (TRM) versus fiber-reinforced polymers (FRP) in shear strengthening of concrete beams" *Composites Part B: Engineering*, Vol 77, pp 338-348, 2015.
  17. T.C. Triantafillou, C.G. Papanicolaou, "Shear strengthening of RC members with textile reinforced mortar (TRM) jackets," *Mater. Struct. RILEM* 39 (1), pp 85–93, 2006.
  18. ABAQUS, "Analysis User's Manual 6.12," Dassault Systèmes Simulia Corp, United States, 2012.
  19. EN 1992-1-1, "Eurocode 2: Design of concrete structures - Part 1-1: General rules and rules for buildings", 2004.

Received: 19.02.2020 Revised: 09.07.2020